bioresources.com

Charring Properties and Temperature Profiles of Laminated Bamboo under Single Side of ISO 834 Fire Exposure

Ming Xu,[a,c,*] Liuhui Tu,[a,b,c] Zhaoyan Cui,[a,b,c] and Zhongfan Chen [a,c]

The charring properties and temperature profiles were studied for laminated bamboo exposed on one-side to ISO 834 fire. A linear model was adopted to represent the charring depth-time relationship. The average charring rate of laminated bamboo was around 1 mm/min, and the charring rate decreased as the total time increased. The temperature of the char front was approximately 270 °C, which was determined *via* analysis of the time-temperature curve. An additional mathematic model was developed to predict the temperature distribution in the uncharred zone under such conditions, and an abrupt change in temperature was witnessed near the char front. When compared to several different timber species found in previous literature and fire resistance standards, the charring rate of laminated bamboo was relatively high; therefore, future research should focus on way to strengthen the fire retardancy of laminated bamboo.

INTRODUCTION

In recent years, laminated bamboo has gained more attention due to its excellent processing performance and mechanical properties (Xiao *et al.* 2012). Previous studies have shown that, like other biological structural materials, laminated bamboo is renewable, sustainable, and also is able to be produced and distributed globally (Yang *et al.* 2009). However, these kinds of material also share disadvantages, such as increased combustibility, which means that they are more flammable than other construction materials under the same circumstances. Research on the fire behavior of laminated bamboo has been limited; therefore unknown barriers and obstacles could interfere with further applications.

Bamboo and timber share a similar chemical constitution, and their microstructures are identical as well, with both being anisotropic and porous polymeric materials with fibrous structures. Therefore, similar research techniques and methods could be applied. Several scholars and experts have already performed studies on the charring rate of timber varieties. Also, certain information could also be gathered from national standards. The fire section of EN 1995-1-2 (2004) is based on the assumption that the charring rate of solid or glued laminated hardwoods decreases with an increase in density, and once the density reaches 450 kg/m^3, the charring rate reaches its limitation of 0.5 mm/min. Research showed

bioresources.com

that the charring rate of Douglas fir varied nonlinearly to time with an average rate of 0.635 mm/min under the standard ISO 834 test (Lawson *et al.* 1952). Computational formulas for the instantaneous and average charring rates were also presented. Charring rates of various timber species are also provided in many design codes and by many other researchers, with their accuracy being guaranteed under certain conditions. According to the investigations of several studies (Babrauskas 2005; Xu *et al.* 2015), the charring rate of certain timber material was constant under both standards, ISO 834 (1999) and ASTM E119-16a (2016), with char rates that ranged from 0.4 mm/min to 0.8 mm/min. For example, raw or laminated pine wood had a char rate of 0.5 mm/min to 0.7 mm/min.

Being a combustible material, the charring properties of wood have been studied by many researchers. The charring rate of wood is affected by many factors such as density, moisture content, external heat flux, and the oxygen concentration of the surrounding environment (Mikkola 1999). A small-scale vertical furnace was used to study the regression expressions of five kinds of wood for ASTM E119 tests, *i.e.* the charring rate, moisture content, density, and char contraction factors (White and Nordheim 1992). Based on the tests of 20 tropical hardwoods exposed to ISO 834 fire resistance testing on one-side, with a density ranging from 421 kg/m^3 to 1080 kg/m^3, a linear regression was developed by Njankouo *et al.* (2004) to express the charring depth over time, showing a strong relationship between the density and the charring rate. The correlation between the charring rate and oxygen permeability has been studied in 12 different wood species, and a summary of the values for the density, charring rate, and oxygen permeability index were gathered from experiments and presented (Hugi *et al.* 2007). Research has shown that engineered bamboo shares similar characteristics to wood, but there are still multiple differences between these materials. When investigating the charring rate and depth of bamboo scrimber, Xu *et al.* (2017) determined, based upon the experimental results, that the charring rate of the bamboo scrimber gradually decreased as the moisture content increased from 6% to 18%. The fire reaction and fire-resistant of *Guadua angustifolia* Kunth bamboo has been determined *via* experiments by Mena *et al.* (2012), and the flame spread results showed that greater energy is required for *Guadua* to propagate fire when compared to plywood; therefore it would be a safer material to utilize for construction applications. Ma *et al.* (2016) described an elementary mechanism for charring and heat-conducting analysis of GluBam laminated bamboo and China fir wood and discovered a similar charring pattern between the two materials. This pattern showed a high charring rate when the specimens were first exposed to high temperature, and it gradually decreased as charring layers began to appear.

The combustion models for wood have been discussed and developed for years by many scholars. The pyrolysis, ignition, and fire spread on the horizontal surface of wood have been studied (Atreya 1983). A model for heat and mass transfer in timber structures during a fire has been developed (Fredlund 1993). These models required numerical calculations, and were often too complicated for practical structural design, so a simplified and analytical model was promoted by Mikkola (1991) to describe the energy balance in the char front of wood during thermal decomposition. Experimental results fit this model well and revealed that the charring rate of wood was influenced greatly by the temperature profile and thermal conductivity of the material. After a surface char layer formed, the low thermal conductivity resulted in a lower heat flux in the char front. Therefore, the total mass loss rate would decrease, which was representative of a lower charring rate. In addition, with a more drastic change of temperature distribution, a faster charring rate was expected to be observed. The thermal conductivity of the wood has been extensively

studied, and the average thermal conductivity, perpendicular to the grain, for a variety of wood species at room temperature was presented by TenWolde *et al*. (1988). For the determination of temperature profiles, a model developed by Frangi *et al*. (2009) was used for the calculation of the temperature in wood members exposed to the standard ISO fire, and when compared with the test results, was found to fit well with the results. For EN 1995-1-2 (2004), the temperature-depth equations were related to the char front temperature, the initial temperature, and the thermal penetration depth of the wood. However, there were also reports that the shrinkage and cracks at the surface of the wood influenced its charring properties and the pyrolysis process. The cracks in the char layer provided greater heat penetration and weaken their protection as heat insulation to the inner layers. The expressions of cracking could be incorporated into pyrolysis models, including the factors of cracks on heat and mass transfer during wood pyrolysis (Shen and Gu 2009). The development of shrinkage and cracks accelerated when the heat flux was increased.

However, for laminated materials the development of cracks has another cause. A specific factor that might play a more important role in the charring properties of laminated bamboo in comparison to other biological materials is the use of construction adhesives. Laminated bamboo use glues, such as phenolic resin, to attach the slices of bamboo together in order to provide the elements with larger cross-sections and increased mechanical properties (Tejado *et al*. 2007). However, its decomposition under high temperatures could lead to layers falling off and a relatively higher charring rate in the material. Frangi *et al*. (2009) found that the fire behavior of the cross-laminated timber panels was strongly linked to the behavior of the adhesive used for bonding the panels, and with the appearance of cracks in the char layers, an increased charring rate was observed. The thermal performance and thermal decomposition of the resins used as a construction adhesive for raw materials has also been studied. Zhang *et al*. (2018) investigated the firing mechanisms of oxide-carbon refractories with a phenolic resin binder, the heat absorption and release, and the weight loss of the binder. The results determined that a temperature between 400 °C to 600 °C represented a critical stage, in which significant weight loss and a decrease in strength would occur. The influence of such thermal decomposition on the fire performance of the laminated bamboo was complex; therefore a relatively direct and straightforward method was required to describe it.

The main objective of this work was to study different factors that may influence the charring rate of the laminated bamboo, such as thickness, the arrangement, grain direction, charring time, and the decomposition of adhesives. The temperature profiles and thermal penetration of the laminated bamboo during the fire are also included. With 4 groups of 20 test specimens exposed to standard ISO 834 (1999) fire resistance testing on one-side *via* controlled heating curves, the results aim to provide references for further studies and applications of laminated bamboo in structural engineering.

EXPERIMENTAL

Test Specimens

Moso bamboo of 4 years old to 5 years old was selected as the raw material for this study, and it was sourced from Fujian, China. The laminated bamboo consisted of longitudinally arranged slender bamboo strips joined with an adhesive. First, the full bamboo culm was cut into pieces. Each piece was split, planed, processed, laminated, and hot-pressed to form the laminated bamboo board product. The hot-press temperature was

120 ± 5 °C. Each strip shared a similar size, with a cross-section of 7 mm × 21 mm. The adhesive used for the laminated bamboo was a water-soluble-impregnated phenolic resin (Dynea Co,. Ltd, Guangdong, China), with a glass transition temperature of approximately 150 °C and was beige colored. The adhesive content of the laminated bamboo was less than 2% of its total mass. The cross-section of the specimens used for charring properties analysis was 300 mm in width and 120 mm in thickness, with a length of 1500 mm.

As shown in Fig. 1, the specimens were exposed to fire perpendicular to their fiber direction, and two kinds of strip arrangements were used, flatwise or edgewise. The charring time was the variable for these 3 control groups, being exposed to fire for either 20 min, 40 min, or 60 min. The three groups were designed to measure the charring properties and the temperature profiles of laminated bamboo. The details of the test specimens are shown in Table 1.

(a) Flatwise   (b) Edgewise
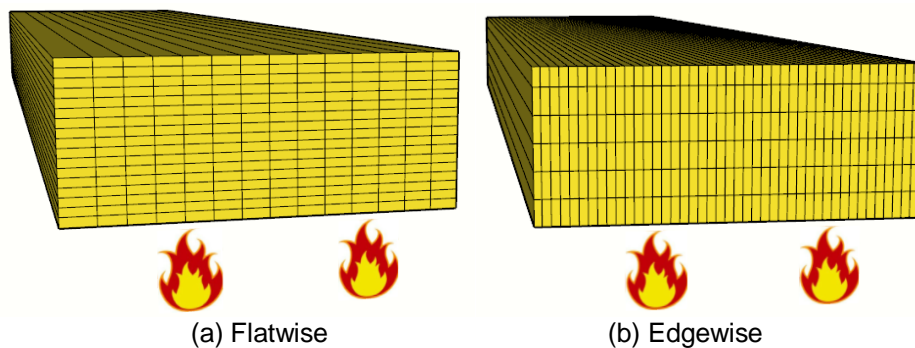
Fig. 1. Strip arrangements of test specimens

Table 1. Test Specimen Conditions

Sample	Strip Arrangement	Exposure Time (min)	Number of Samples
F20		20	2
F40	Flatwise	40	2
F60		60	2
E20		20	2
E40	Edgewise	40	2
E60		60	2
F denotes flatwise direction and E denotes edgewise direction			

Table 2. Thermal Properties of the Laminated Bamboo

Temperature (°C)	Density Ratio	Specific Heat (KJ/(kg·K))	Thermal Conductivity (W/(m·K))
20	1.00	1.30	0.134
50	0.95	1.55	0.174
90	0.94	2.32	0.195
150	0.93	1.08	0.138
200	0.92	1.03	0.099
250	0.86	1.00	0.087
280	-	-	0.071
300	0.66	1.15	-
350	0.36	1.42	-
400	0.30	1.00	-

bioresources.com

The thermal properties of the laminated bamboo were determined according to ASTM E 1269-11 (2011), as shown in Table 2. The physical properties in Table 3 were determined *via* the same testing methods.

Table 3. Physical Properties of the Test Specimens

Physical Property	Fluctuation Range	Average Value	Standard Deviation	Coefficient of Variation
Air-Dry Density (kg/m^3)	536 to 698	609	59.9	9.82%
Oven-Dry Density (kg/m^3)	517to 665	592	58.0	9.80%
Moisture Content (%)	4.80 to 6.47	5.90	0.059	14.48%

Test Methodology

The one-sided fire test was carried out in a small horizontal furnace with temperature-time exposures according to the ISO 834 (1999) methodology. The furnace dimension was 1800 mm in length, 1200 mm in width, and 500 mm in depth. The details of the small horizontal furnace are shown in Fig. 2.

(a) Small horizontal furnace   **(b)** Plane section
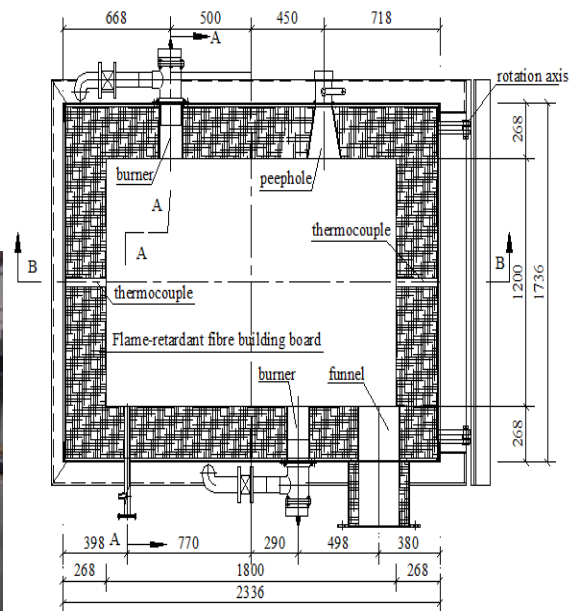
(c) A-A cross-section   **(d)** B-B cross-section
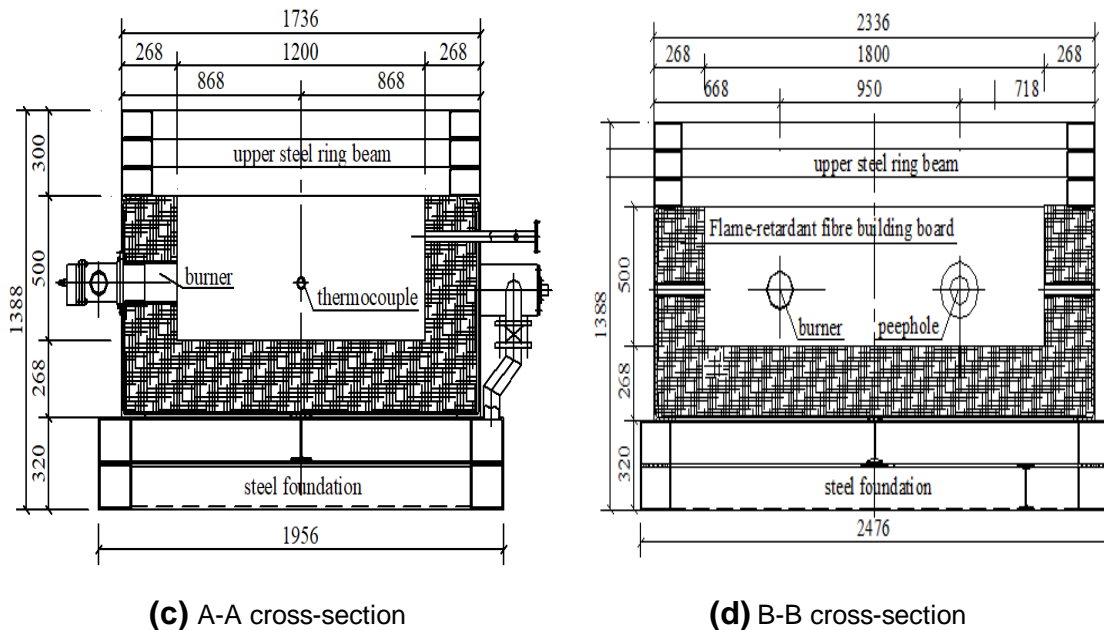
Fig. 2. Details of small horizontal furnace

Because the test exposed the sample to fire only on one side, the upper surface of the laminated bamboo needed to be exposed outside the furnace. Two specimens were fired at the same time for each fire test. The furnace surface was covered by the furnace cover, except where the bamboo plate was positioned. Rock wool was used to fill the gap between the furnace cover and the bamboo plate to ensure that no smoke would overflow during the test. A rope connecting the steel wires at both ends of the bamboo plate was used to immediately lift the sample at the end of the test, and the fire was extinguished with water. The specimen was placed outside to dry until further analysis could be performed. The test setup and the placement of the test specimens are shown in Fig. 3. The temperature of the measuring point was obtained through a thermocouple with an acquisition frequency of 50 Hz. The fuel source used was natural gas and the temperature of the furnace was measured *via* type K thermocouples.
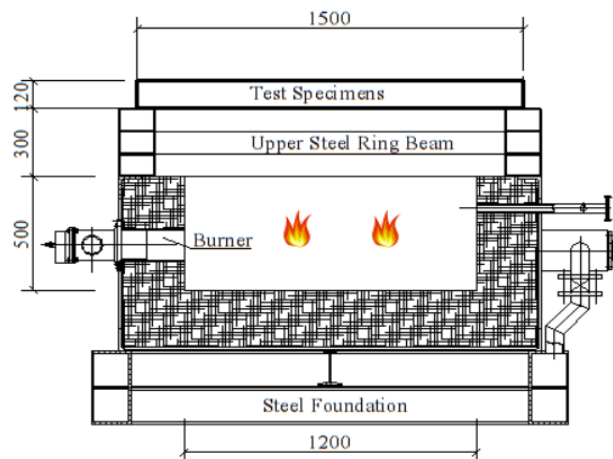
Fig. 3. Details of the small horizontal furnace

As shown in Fig. 4, 10 thermocouples were placed at different distances from the exposed surfaces of each one of the laminated bamboo specimens under 60 min of fire. There were only 2 specimens being placed with thermocouples, F60-1 being flatwise arrangement and E60-1 being edgewise arrangement. From furthest to closest, the distances were 50 mm, 40 mm, 30 mm, 20 mm, and 10 mm. Test holes were added in accordance to the design depth before the experiment and were fully filled with bamboo dust after the thermocouples were placed in the holes. Two typical thermocouples were set to measure the environmental temperature, and the temperature-time curves recorded by the computer were identical to the temperature-time curves shown in ISO 834 (1999).

(a) Distribution of thermocouples (Top view)

(b) Distribution of thermocouples (Sectional view)
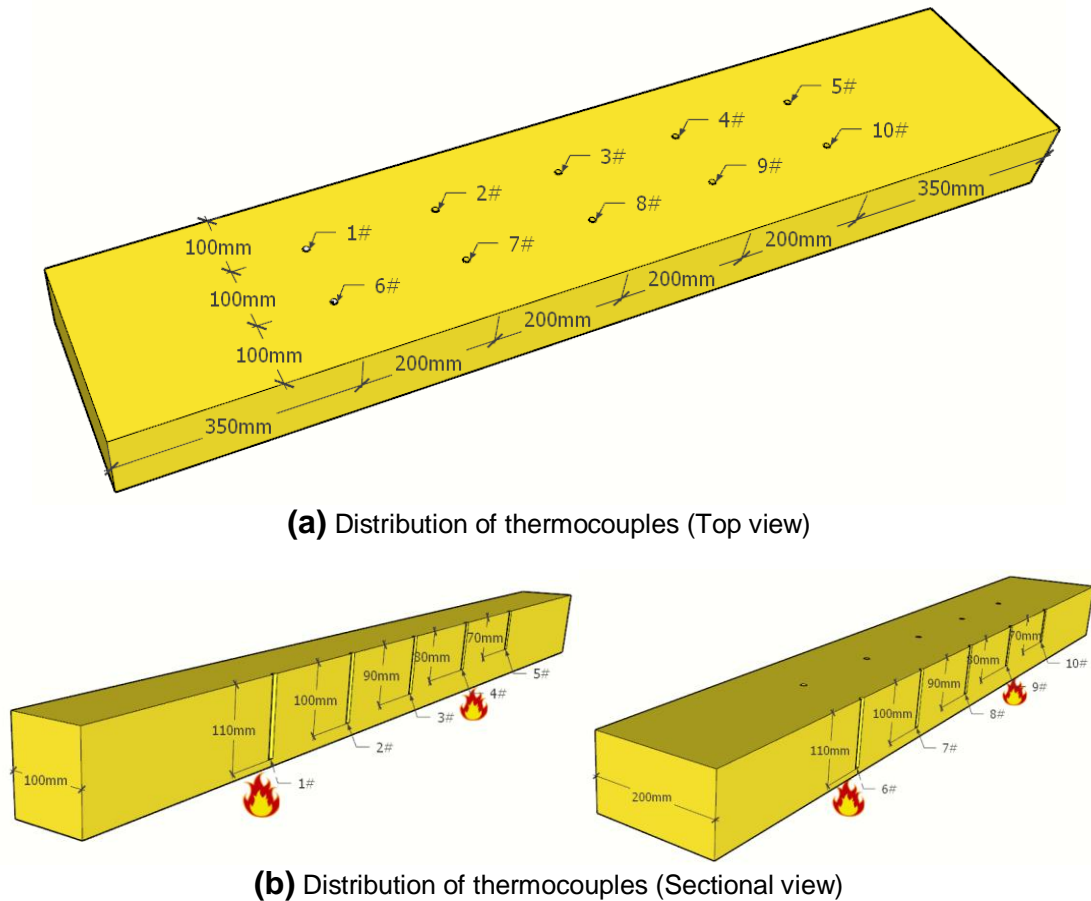
Fig. 4. Positions of the test points

RESULTS AND DISCUSSION

The furnace temperature during the test was recorded *via* thermocouples, and the temperature-time curve was shown in Fig. 5.

Charring Properties

As shown in Fig. 6, two types of cracks appeared on the surface of the test specimens after testing, one being cracking along with the bonding gaps, and another being the fractures of bamboo strips. The samples that wee arranged edgewise showed more

cracks after testing because there more glue lines exposed to fire than another strip arrangement.
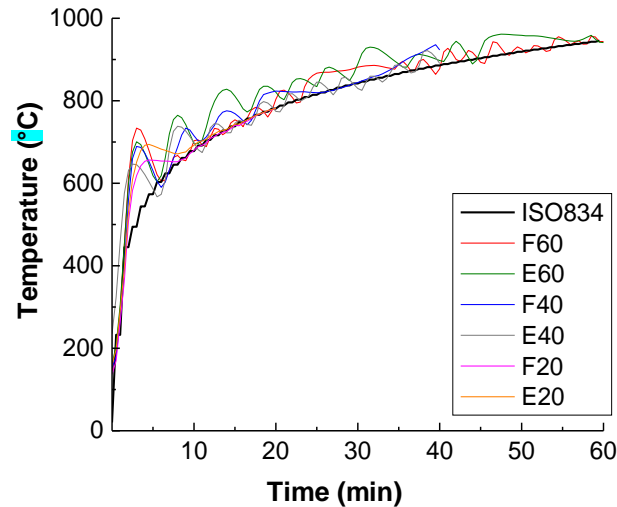
Fig. 5. Temperature-time curve of the test furnace

(a) Flatwise Arrangement(Top view)

(b) Edgewise Arrangement(Top view)

(c) Flatwise Arrangement(Detail view)

(d) Edgewise Arrangement(Detail view)

Fig. 6. Char layer of the test specimens

When the fire exposure test was over, the test specimens were removed from the horizontal furnace, and the fire on the specimens was extinguished immediately with water. After the specimens cooled down, part of the test member was taken and was cut into halves along the vertical direction. The char layers attached to the specimens were scraped, and the residual cross-sections of the upper specimens were measured using a Vernier caliper with 3 measurement positions, *e.g.* 50 mm, 75 mm, and 100 mm from one side of the

specimen. By measuring the remaining thickness of the test members in 3 different places, the charring depth equaled the loss of thickness and the detailed data was shown in Table 4.

Table 4. Test Results of the Charring Properties

Sample	Charring Depth (mm)	Charring Rate (mm/min)	Average Charring Rate (mm/min)
F20-1	19.0	0.95	0.95
F20-2	19.0	0.95	
F40-1	40.0	1.00	0.95
F40-2	36.0	0.90	
F60-1	58.8	0.98	1.03
F60-2	64.8	1.08	
E20-1	19.0	0.95	0.98
E20-2	20.2	1.01	
E40-1	37.2	0.93	0.90
E40-2	34.8	0.87	
E60-1	61.2	1.02	1.05
E60-2	64.8	1.08	

As shown in Table 4, the charring depth gradually rose as the charring time increased and the charring rate became greater in the last 20 min.

To analyze the change regulation of the charring depth by time, based on the real experiment situation determined by White and Nordheim (1992), a linear model was adopted to represent the charring rate-time relationship, as shown by Eq 1.,

$$x_c = 0.98t \tag{1}$$

where x_c is the charring depth under a single side of fire exposure and t is the charring time. A comparison between the calculations based on the equation and the experimental results are presented in Table 5. There was no relative difference larger than 15%, which meant that this model was well fit.

Table 5. Comparison of the Charring Depth of Laminated Bamboo

Sample	Time (min)	Experimental Results (mm)	Calculated Results (mm)	Relative Difference (%)
F20-1	20	19.00	19.60	3.16%
F20-2	20	19.00	19.60	3.16%
F40-1	40	40.00	39.20	-2.00%
F40-2	40	36.00	39.20	8.89%
F60-1	60	58.80	58.80	0.00%
F60-2	60	64.80	58.80	-9.26%
E20-1	20	19.00	19.60	3.16%
E20-2	20	20.20	19.60	-2.97%
E40-1	40	37.20	39.20	5.38%
E40-2	40	34.80	39.20	12.64%
E60-1	60	61.20	58.80	-3.92%
E60-2	60	64.80	58.80	-9.26%

A comparison between the charring rate of laminated bamboo and similar wood product (Njankouo *et al.* 2004) and bamboo scrimber (Xu *et al.* 2018) is shown in Table 6. With a moisture content of 5.90% and a of density was approximately 600 kg/m³, the

bioresources.com

charring rate of the laminated bamboo was greater than the rate for other species. This might be caused by the relatively lower moisture content of the laminated bamboo and the cracks that appeared on the surface during the test. In addition, the data in Table 6 showed that the density had a major effect on the charring rate.

Table 6. Comparison of the Charring Rates of Different Species

Species	Moisture Content (%)	Density (kg/m³)	Charring Rate (mm/min)
Spruce	9	480	0.62
Fir	13	421	0.71
Oak	10	557	0.59
Wenge	13	923	0.49
Afzelia	12	800	0.51
Bilinga	11	692	0.58
Merbau	12	779	0.50
	10	522	0.54
Meranti	10	522	0.55
Glued Laminated Hardwood (EC 5)	-	≥ 450	0.50
Softwood and Beech (EC 5)	-	≥ 290	0.65
Douglas Fir from China	16.3	450	0.84
Bamboo Scrimber	6	1018	0.47
Laminated Bamboo	5.9	609	0.98

Temperature-Time Curves

Figure 5 shows the furnace temperature curve under each test condition. Compared to the ISO 834 (1999) heating curve, the average furnace temperature increase curve of each test was consistent with the standard.

As shown in Fig. 7, during the fire test, the temperatures at the measuring points increased with time. At the initial warming section stage, the temperature rose from normal temperature to 100 °C, and the temperature-time relationships were linear. The temperature increase rate decreased at this stage as the distance from the fire surface increased. Then the temperature became stable at approximately 100 °C. Due to the evaporation of the moisture in the test specimen, the temperature curve of the measuring point produced a distinct platform section. However, after the moisture was fully evaporated, the temperature continued to increase.

From previous research, Frangi *et al.* (2009) reported the temperature of the char front as 253 °C, while Schaffer *et al.* (1992) gave a temperature of 288 °C and 360 °C, respectively. Based on these, a conclusion could be drawn that the temperature of the char front was between 250 °C and 300 °C, which was where the pyrolysis zone was located. The starting point of this stage represented the complete carbonization of the material, but the charred layer at the corresponding position had not been cracked, and the endpoint represented material that was not completely carbonized. Xia *et al.* (2017) stated that the temperature of the char front of laminated bamboo was 270 °C, and in this study, further analysis was based upon that temperature.

After the test points' temperatures rise beyond 270 °C, the cracks on the surface begin to develop deeper into the test specimens. The heat is able to penetrate into the

specimens along with the cracks. The thermocouples were gradually exposed to the outside of the material. A rapid rise of temperature has been captured by the test points. After that, the temperature curve was similar to the furnace temperature curve.
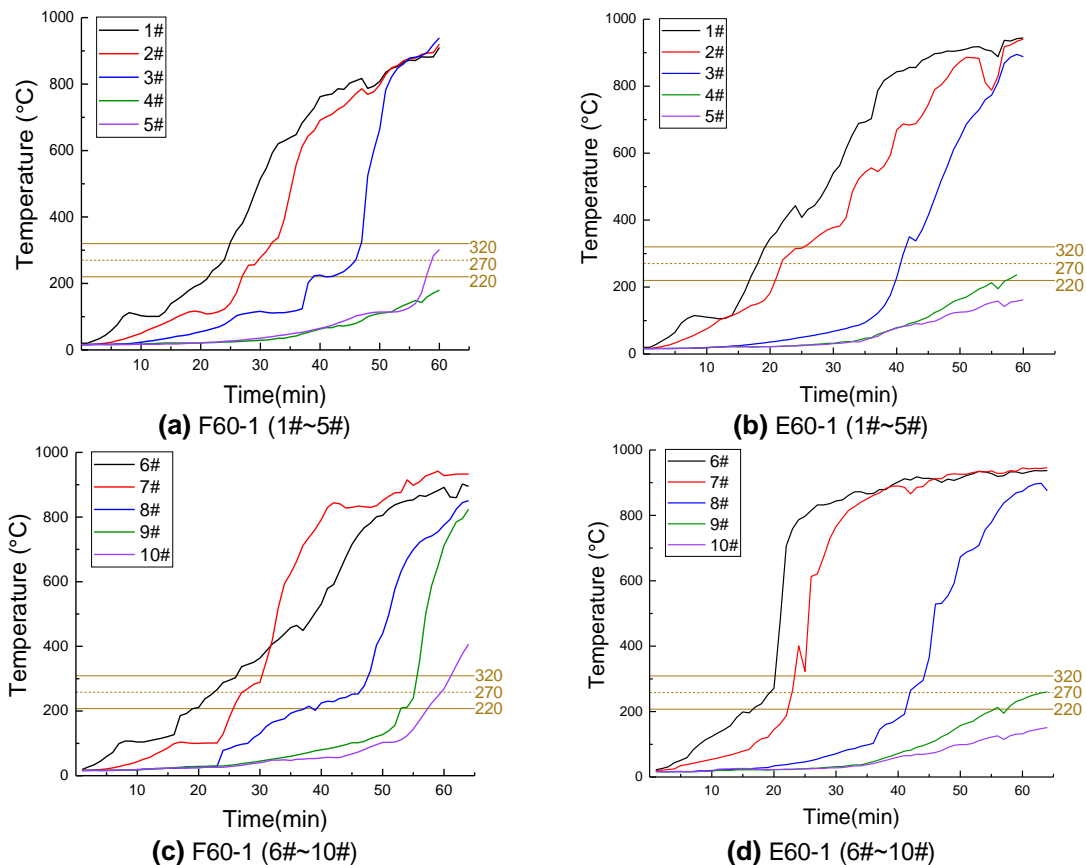
Fig. 7. Time-temperature curves of measuring points

Because it is closer to the surface of the fire, the evaporation of water showed a greater influence on the phenomenon of the platform segment. In addition, this phenomenon is more clearly observed at the test points closer to the surface of the fire. This is because the water in the inner layer also evaporated during the heating process. The water evaporation process took a long time, so the phenomenon was less obvious with the further away test points.

Temperature Profiles

As can be seen from the pyrolysis models previously mentioned, the temperature development in wood greatly influenced the charring rate of the wood.

As described by EN 1995-1-2 (2004), the temperature-depth equations of the wood are shown in Eq. 2,

$$T(x) = 20 + 180(1 - \frac{x}{25})^2 \tag{2}$$

where T represents the wood temperature (°C) as a function of the depth and x is the depth (mm) measured from the char front. Thermal penetration depth is defined as the distance from the char-line to the part of wood at room temperature. For standard EN 1995-1-2 (2004) the thermal penetration depth was defined as 40 mm. A range of 40 mm to 50 mm

was purposed by Mikkola (1991), and Lache (1992) reported it as 25 mm.

Kordina *et al*. (1994) used the following equations to predict the temperature profile of wood exposed to ISO fire resistance testing on one-side, as shown in Eqs. 3 and 4,

$$T(x) = 20 + 180(1 - \frac{\beta t}{x + \beta t})^\alpha \qquad (3)$$

$$\alpha(t) = 0.398 t^{0.62} \qquad (4)$$

where β is the charring rate (mm/min). Frangi and Fontana (2003) mentioned that when the calculated results from the equations were compared with their experimental values, the standard model in EN 1995-1-2 (2004) did not give a good prediction of the temperature profile for long fire durations. The main reason was the assumption that the thermal penetration depth (25 mm) does not change with time and the surrounding environment. In particular, for long fire durations, these calculation models are often inaccurate, as their predicted temperature profiles tend to be lower than the measured ones. Frangi and Fontana (2003) provided a new calculation model by modifying the expression of α, as shown in Eqs. 5 and 6,

$$T(x) = 20 + 180(\frac{\beta t}{x + \beta t})^\alpha \qquad (5)$$

$$\alpha(t) = 0.025 t + 1.75 \qquad (6)$$

where the variables were the same as defined in previous equations.
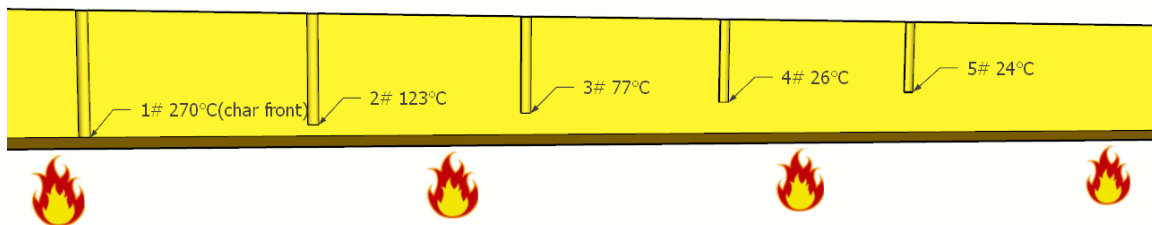
Fig. 8. The analysis method of the temperature distribution

To analyze the temperature profile of the laminated bamboo, the test results were compared with the calculation predictions for all three models. The test specimens for the temperature profile test were all perpendicular to the grain, with two groups in the flatwise orientation and two groups in the edgewise orientation. For the temperature-time curve obtained from the 60 min fire exposure test, differences in the temperature distribution between each test point were observed. In the first group of flatwise specimens, once the temperature reached 270 °C at the test point 10 mm away from the fire exposure surface, the temperatures of the test points 20 mm, 30 mm, 40 mm, and 50 mm away from the surface were 123 °C, 77 °C, 26 °C, and 24 °C, respectively, as shown in Fig. 8.

The same method was applied to each group at the test points 20 mm, 30 mm, 40 mm, and 50 mm from the surface when they reached 270 °C. An additional assumption here used the depth of the test point from the surface to replace βt when the measured temperature reached 270 °C. The mean results of 1#~5# and 6#~10# in each group were taken for further temperature profile analysis. The test results are presented in Table 7.

Table 7. Experiments Results of the Laminated Bamboo

Strip Arrangement	Charring Depth (mm)	Time (min)	Depth From Char Front (mm)	Temperature (°C)
Flatwise	10	24	10	123
			20	77
			30	26
			40	24
	20	30	10	116
			20	35
			30	29
	30	46	10	102
			20	80
Edgewise	10	18	10	150
			20	31
			30	22
			40	20
	20	22	10	41
			20	24
			30	23
	30	41	10	82
			20	66

By comparing the test results with the theoretical prediction of each model, the deviations of each model are shown in Table 8.

Table 8. Deviation of Each Calculation Model

Flatwise Arrangement				
Depth From Surface (mm)	Depth From Char Front (mm)	EC Deviation	HBH Deviation	A.F. & M. F. Deviation
10	10	-31.06%	-63.51%	-55.04%
	20	-64.68%	-63.87%	-56.34%
	30	-35.24%	-44.19%	3.65%
	40	253.33%	-9.09%	0.41%
20	10	-26.90%	-41.69%	-26.45%
	20	-54.67%	-35.75%	3.96%
	30	-6.21%	-0.26%	31.77%
30	10	-64.67%	-69.73%	49.20%
	20	-66.00%	-49.64%	-23.85%
Edgewise Arrangement				
Depth From Surface (mm)	Depth From Char Front (mm)	EC Deviation	HBH Deviation	A.F. & M. F. Deviation
10	10	-76.00%	-63.75%	-60.55%
	20	-19.35%	6.61%	16.31%
	30	50.00%	20.75%	29.66%
	40	100.00%	19.26%	26.09%
20	10	-65.85%	95.38%	121.55%
	20	-4.17%	98.34%	135.63%
	30	47.83%	52.58%	82.08%
30	10	-75.61%	-5.74%	23.19%
	20	-46.97%	-33.98%	-3.61%
EC: EN 1995-1-2 (2004); HBH: Kordina *et al.* (1994); A.F. & M. F.: Frangi *et al.* (2003)				

By analyzing Fig. 7 and the calculation results, two primary conclusions could be drawn, as follows: (1) The calculation model purposed by Frangi and Fontana (2003) was found to be accurate when it came to the prediction of temperature profiles of laminated bamboo subjected to a long charring duration and exhibited a char line depth relatively greater than 30 mm. This was due to the simplified calculation model in EN 1995-1-2 (2004) not accurately predicting the temperature profiles for samples subjected to a long fire duration and for the simplified assumption of a predetermined thermal penetration depth of 25 mm. In addition, the theoretical profiles of long fire duration from the Holz Brandschutz Handbuch (Kordina *et al*. 1994) were lower than the test temperature profiles, which meant that this model was not accurate in this circumstance. The adjustment of the model made by Frangi and Fontana (2003) focused on a longer fire duration *via* the combination of the total fire exposure time with α, which yielded a new model with greater accuracy. (2) The temperature profiles of the laminated bamboo showed great discreteness. All the predictions could not accurately predict the temperature profiles of positions close to the char front. The predictions were all lower than measured temperatures; therefore, a new model was required for this special bio-material.

The new calculation model for laminated bamboo was based on the model created by Frangi and Fontana (2003). Given its accuracy in predicting temperature profiles subjected to a long total fire duration, and being far from the char front, the adjustment was to amplify the theoretical temperature in order to secure accuracy. The lack of experimental data should be taken into consideration for usage of the new model for samples with a depth measurement far from the char line.

The following equations were developed to calculate the temperature profile in a wood member subjected ISO fire resistance testing on a single side, as shown in Eq. 7. In Eq. 8., the heat has been considered only penertrated 40 mm un depth behind the char front. Therefore:

$$T(x) = 20 + 250(1 - \frac{x}{40})^\alpha \tag{7}$$

$$\alpha(t) = at + b \tag{8}$$

The relationship between $\alpha(t)$ and t could be described through linear fit (Table 9),

Table 9. The Linear Relationship between $\alpha(t)$ and t

Flatwise	$\alpha(t)$	2.80	3.37	3.83	linear	$\alpha(t) = 0.0434$	R²	0.9025
Arrangement	t	24	30	46	fit	$t + 1.8856$		
Edgewise	$\alpha(t)$	3.65	4.54	5.09	linear	$\alpha(t) = 0.0518t$	R²	0.7745
arrangement	t	18	22	41	fit	$+ 3.0285$		

where the value of *a* and *b* is 0.0434 and 1.8856 for flatwise specimens. As for edgewise specimens, *a* is 0.0518 and *b* is 3.0285. Table 10 showed the comparison between the test results and the new calculation model, and almost all the prediction results showed deviation less than 10%.

Table 10. Deviation of the New Calculation Model

Flatwise Arrangement			
Depth From Surface (mm)	Depth From Char Front (mm)	$T(x)$ (°C)	New Calculation Model Deviation
10	10	131.84	3.24%
	20	56.00	5.93%
	30	25.18	3.53%
	40	20.00	0.00%
20	10	114.82	-4.26%
	20	44.18	-6.87%
	30	22.34	-2.92%
30	10	102.97	1.12%
	20	37.53	1.55%
Edgewise Arrangement			
Depth From Surface (mm)	Depth From Char Front (mm)	T(x) (°C)	New Calculation Model Deviation
10	10	110.76	10.76%
	20	38.95	8.03%
	30	21.44	1.94%
	40	20.00	0.00%
20	10	87.76	-7.98%
	20	30.76	-9.28%
	30	20.46	-1.51%
30	10	77.83	1.36%
	20	27.35	1.18%

When the calculated results were compared to the measured temperature, it was shown that the new calculation model gave a more accurate prediction. Considering the high level of discreteness that the temperature profiles of the laminated bamboo showed, the new model guaranteed accuracy; therefore, the development of this calculation method based on the standard EN 1995-1-2 (2004) and research by Frangi *et al*. (2003) was appropriate.

CONCLUSIONS

1. The average charring rate of laminated bamboo was approximately 1 mm/min.

2. With consideration of the influence of water evaporation and other factors, the temperature of the measuring point increased with time, and the curve trends could be divided into several stages.

3. Both test specimens with grain directions perpendicular to the fiber direction were tested, and no major difference was witnessed. Based on the experimental results and the mathematical analysis, suggestions for the application of this biological construction material were proposed.

4. The experimental results showed that in the uncharred zone, an abrupt change in temperature was witnessed, as an approximate 150 °C drop in 10 mm from the char front was observed.

bioresources.com

5. A mathematic model for the analysis of the temperature profiles of laminated bamboo was presented. Compared to the temperature profiles of other timber materials, similar temperature distributions were calculated. Mathematical models for timber materials developed by other researchers had a good fit with laminated bamboo samples with a 10 mm to 40 mm distance from the char front.

ACKNOWLEDGMENTS

Declaration of Conflicting Interest
The authors declare no conflict of interest.

REFERENCES CITED

ASTM E119-16a (2016). "Standard test methods for fire tests of building construction and materials," ASTM International, West Conshohocken, PA.

ASTM E1269-11 (2011). "Standard test method for determining specific heat capacity by differential scanning calorimetry," ASTM International, West Conshohocken, PA.

Atreya, A. (1983). *Pyrolysis, Ignition, and Fire Spread on Horizontal Surfaces of Wood*, Ph. D. Dissertation, Harvard University, Cambridge, MA.

Babrauskas, V. (2005). "Charring rate of wood as a tool for fire investigations," *Fire Safety Journal* 40(6), 528-554. DOI: 10.1016/j.firesaf.2005.05.006

EN 1995-1-2 (2004). "Eurocode 5: Design of timber structures-Part 1-2: General - Structural fire design," European Committee for Standardization, Brussels, Belgium.

Frangi, A., and Fontana, M. (2003). "Charring rates and temperature profiles of wood sections," *Fire and Materials* 27(2), 91-102. DOI: 10.1002/fam.819

Frangi, A., Fontana, M., Hugi, E., and Jübstl, R. (2009). "Experimental analysis of cross-laminated timber panels in fire," *Fire Safety Journal* 44(8), 1078-1087. DOI: 10.1016/j.firesaf.2009.07.007

Fredlund, B. (1993). "Modelling of heat and mass transfer in wood structures during fire," *Fire Safety Journal* 20(1), 39-69. DOI: 10.1016/0379-7112(93)90011-E

Hugi, E., Wuersch, M., Risi, W., and Wakili, K. G. (2007). "Correlation between charring rate and oxygen permeability for 12 different wood species," *Journal of Wood Science* 53(1), 71-75. DOI: 10.1007/s10086-006-0816-1

ISO 834 (2012). "Fire resistance tests-elements of building construction," International Organization for Standardization, Geneva, Switzerland.

Kordina, K., Meyer-Ottens, C., and Scheer, C. (1994). "Holz Brandschutz Handbuch, Deutsche Gesellschaft für Holzforschung eV," München, 2.

Lache, M. (1992). "Untersuchungen zur Abbrandgeschwindigkeit von Vollholz und zur Feuerwiderstandsdauer biegebeanspruchter," *BSH-Träger*. Institut für Holzforschung der Universität München.

Lawson, D. I., Webster, C., T., and Ashton, L. A. (1952). "The fire endurance of timber beams and floors," *The Structural Engineer* 30(2), 27-34.

Ma, J.-F., Huo, J.-S., and Xiao, Y. (2016) "Experimental study on the charring rate and temperature field of the Glubam exposed to the one-sided flame," *Journal of Safety and Environment* 5, 168-172.

Mena, J., Vera, S., Correal, J. F., and Lopez, M. (2012). "Assessment of fire reaction and fire resistance of *Guadua angustifolia* kunth bamboo," *Construction and Building Materials* 27(1), 60-65. DOI: 10.1016/j.conbuildmat.2011.08.028

Mikkola, E. (1991). "Charring of wood based materials," *Fire Safety Science* 3, 547-556. DOI: 10.3801/IAFSS.FSS.3-547

Njankouo, J. M., Dotreppe, J.-C., and Franssen, J.-M. (2004). "Experimental study of the charring rate of tropical hardwoods," *Fire and Materials* 28(1), 15-24. DOI: 10.1002/fam.831

Shen, D. K., and Gu, S. (2009). "The mechanism for thermal decomposition of cellulose and its main products," *Bioresource Technology* 100(24), 6496-6504. DOI: 10.1016/j.biortech.2009.06.095

Tejado, A., Peña, C., Labidi, J., Echeverria, J. M., and Mondragon, I. (2007). "Physico-chemical characterization of lignins from different sources for use in phenol–formaldehyde resin synthesis," *Bioresource Technology* 98(8), 1655-1663. DOI: 10.1016/j.biortech.2006.05.042

TenWolde, A., McNatt, J. D., and Krahn, L. (1988). *Thermal Properties of Wood and Wood Panel Products for Use in Buildings* (Report No. DOE/USDA-21697/1; ORNL/Sub-87-21697/1), U.S. Department of Agriculture Forest Products Laboratory, Madison, WI.

White, R., and Nordheim, E. (1992). "Charring rate of wood for ASTM E119 exposure," *Fire Technology* 28(1), 5-30. DOI: 10.1007/BF01858049

Xia, Q. X. (2017). *Experimental Study on Basic Properties of Laminated Bamboo at High Temperature*, Master's Thesis, Southeast University, Nanjing, China.

Xiao, Y., and Ma, J. (2012). "Fire simulation test and analysis of laminated bamboo frame building," *Construction and Building Materials* 34, 257-266. DOI: 10.1016/j.conbuildmat.2012.02.077

Xu, M., Cui, Z., Chen, Z., and Xiang, J. (2017). "Experimental study on compressive and tensile properties of a bamboo scrimber at elevated temperatures," *Construction and Building Materials* 151, 732-741. DOI: 10.1016/j.conbuildmat.2017.06.128

Xu, M., Cui, Z., Chen, Z., and Xiang, J. (2018). "The charring rate and charring depth of bamboo scrimber exposed to a standard fire," *Fire and Materials* 42(7), 750-759. DOI: 10.1002/fam.2629

Xu, Q., Chen, L., Harries, K. A., Zhang, F., Liu, Q., and Feng, J. (2015). "Combustion and charring properties of five common constructional wood species from cone calorimeter tests," *Construction and Building Materials* 96, 416-427. DOI: 10.1016/j.conbuildmat.2015.08.062

Yang, T.-H., Wang, S.-Y., Tsai, M.-J., and Lin, C.-Y. (2009). "The charring depth and charring rate of glued laminated timber after a standard fire exposure test," *Building and Environment* 44(2), 231-236. DOI: 10.1016/j.buildenv.2008.02.010

Zhang, J., Mei, G., Xie, Z., and Zhao, S. (2018). "Firing mechanism of oxide-carbon refractories with phenolic resin binder," *Ceramics International* 44(5), 5594-5600. DOI: 10.1016/j.ceramint.2017.12.206